2 THEORETICAL BACKGROUND

2.1 Analysis

Analysis methods can be categorized into classical and numerical approaches. The classical approach involves finding stress or displacement solutions that satisfy the differential equations of equilibrium, compatibility requirements as well as stress-strain relationships, subject to the given boundary conditions. Due to these stringent requirements, very few classical solutions are available for practical plate bending problems.

This difficulty can be overcome by approximating plate behaviour with a crossing beam analogy such as the equivalent frame method, Corley and Jirsa (1970). The results of such an equivalent frame analysis, as well as the required reinforcement, are assumed known in the hand-calculation method presented in 3.1.1.

Numerical approaches require discretisation of the problem, i.e. a structure with an infinite number of degrees of freedom is reduced to a finite number to simplify the calculation process. Two of the best known methods are the method of finite differences and the finite element method. The method of finite differences has the disadvantage of difficulty in satisfying irregular boundary conditions. The finite element method, which is the method of choice in this dissertation, is presented in section 2.1.2.

2.1.1 Hand-Calculation Method

Short and long term deflections of two way slab systems can be calculated by the simplified method outlined below. This method is recommended by various authors, such as Gilbert (1988), Ghali and Favre (1986), as well as the ACI 318 (1999).

For flat slabs, the method involves calculating the mid-span deflections of the middle strip relative to the column strip deflections, x and y-direction strips being treated independently. The middle strip deflections are then added to the average of the column strip deflections and finally, the x and y-direction mid-span deflections are averaged to arrive at a total mid-panel deflection.

The deflection calculations outlined above, make use of known curvatures which are modified with factors to account for cracking, shrinkage and creep. These factors are discussed in detail in sections 3.2 through 3.4.

The main drawbacks of the method are as follows:

- Only rectangular slabs are considered,
- Bending moment magnitudes are assumed to be known, although these moments can easily be calculated using the Direct Design (ACI 318, 1999) or Equivalent Frame Methods,
- Curvatures are assumed to be parabolically distributed over the length of the strip considered,
- Simple support or continuity is assumed.

Deflection at the centre of a strip is given by (Ghali & Favre, 1986):

$$\delta = \frac{l^2}{96}(\psi_1 + 10\psi_2 + \psi_3) \qquad (2.1)$$

where:

l = length of the strip

ψ_1, ψ_2, ψ_3 = curvatures at the left support, centre and right support of the strip.

Deflection at the centre of a panel can be expressed as the sum of the middle strip deflection and the average of the column strip deflections.

$$D_1 = \delta_{EF} + \frac{1}{2}(\delta_{AB} + \delta_{DC}) \qquad (2.2)$$

$$D_2 = \delta_{HI} + \frac{1}{2}(\delta_{AD} + \delta_{BC}) \qquad (2.3)$$

$$D_{final} = \tfrac{1}{2}(D_1 + D_2) \qquad (2.4)$$

The various deflection components in the equations (2.2) through (2.4) are illustrated in figure 2-1.

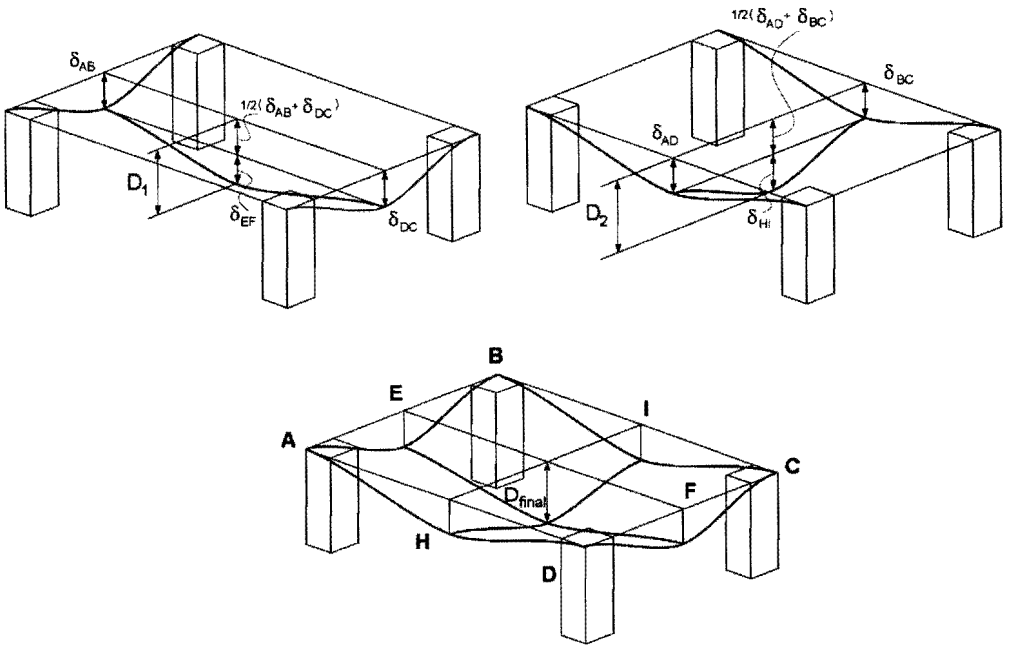

Figure 2-1: Displacement components

Curvature and bending moment can be related with the following equations (Ghali & Favre, 1986):

$$\psi_x = \frac{1}{E_c I_g}\left(M_x + \nu M_y\right) \tag{2.5}$$

$$\psi_y = \frac{1}{E_c I_g}\left(M_y + \nu M_x\right) \tag{2.6}$$

$$I_g = \frac{h^3}{12\left(1-\nu^2\right)} \tag{2.7}$$

where:

E_c = Young's modulus of the concrete,

I_g = Effective moment of inertia of the gross concrete area of the strip,

M_x, M_y = Moments at the section under consideration,

ν = Poisson's ratio of the concrete (usually taken as 0.2),

h = Slab thickness.

2.1.2 Finite Element Method

This method involves the discretisation of continua problems into finite sub regions termed finite elements. The approach yields approximate results based on an assumed stress field, displacement field or a mixed, hybrid approach. These fields are defined by points, or nodes, in the finite element. The approach presented here is limited to the displacement approach, due to its widespread use for matrix analysis software.

The element used in the study is an eight-noded Serendipity element. These elements differ from elements such as Lagrange elements in the derivation of their shape functions. Langrage elements can contain nodes interior to the element and the Lagrange interpolation function is used to find these shape functions. Serendipity elements on the other hand, usually consist of only edge nodes and the shape functions are found by inspection.

Shape functions are approximations of element geometry and deflection behaviour. The same shape functions (second degree polynomials) are used for the definition of geometry and displacement, classifying this element as parabolic isoparametric.

The assumptions for the flexural formulation, due to Mindlin (1951), are as follows:

- The lateral deflection of the plate is small compared to its plan dimensions.
- Planes normal to the plate mid-surface remain plane, but not necessarily normal to the mid-surface, after bending.
- Stresses normal to the plate mid-surface are negligible.

The Kirchhoff, or thin-plate, assumptions (Ugural, 1999) for plate bending differ only in the second point above: Planes remain plane *and* normal to the mid-surface after bending. This implies that the Kirchhoff model neglects shear effects.

The Mindlin elements were developed mainly to overcome inter-element continuity problems that arose from the use of their Kirchhoff counterparts. Mindlin elements do pose some numerical problems such as "shear locking" which is elaborated upon at the end of this section.

The generalised displacements of the plate are completely described using three degrees of freedom per node where w denotes a displacement in the z direction and θ_x and θ_y orthogonal rotations about the y and x axis, respectively. This leads to following expressions for the plate deformations

$$\{\delta\} = \begin{bmatrix} w \\ \theta_x \\ \theta_y \end{bmatrix} = \begin{bmatrix} w \\ \dfrac{\partial w}{\partial x} + \phi_x \\ \dfrac{\partial w}{\partial y} + \phi_y \end{bmatrix} \tag{2.8}$$

These physical quantities and the orientation of the global Cartesian coordinate system are illustrated in figure 2-2.

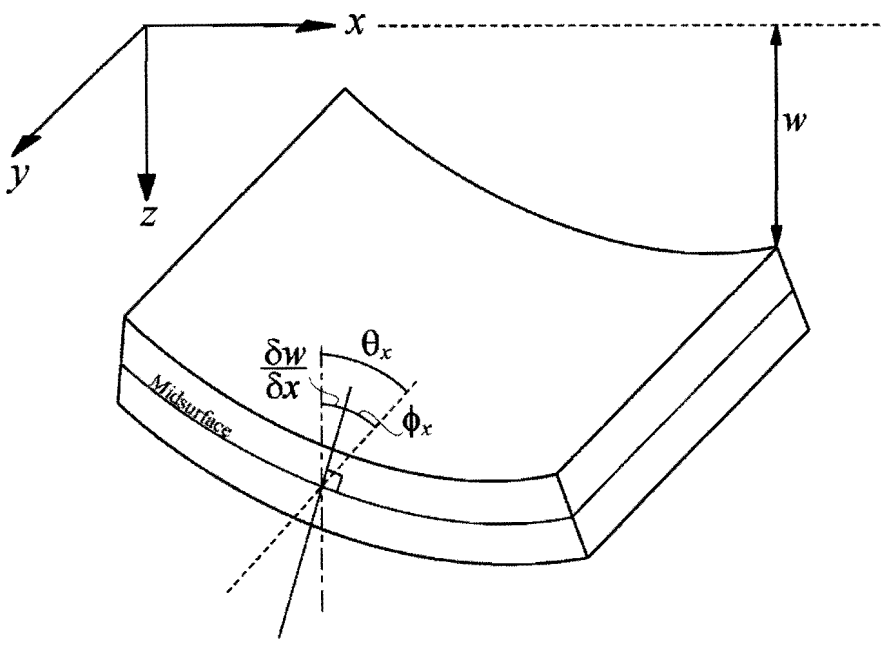

Figure 2-2: Plate deformations

The formulation makes use of a natural (dimensionless), curvilinear coordinate system in ξ and η with origin at the geometric centre of the element. Although the directions of the ξ and η axes vary within the element, the general positive directions are:

- Positive ξ is taken in the same direction as indicated by the nodal sequence 1-2-3.
- Positive η is taken in the same direction as indicated by the nodal sequence 3-4-5.

The nodal numbering starts at any corner of the element and proceeds in an anti-clockwise direction as shown in figure 2-3.

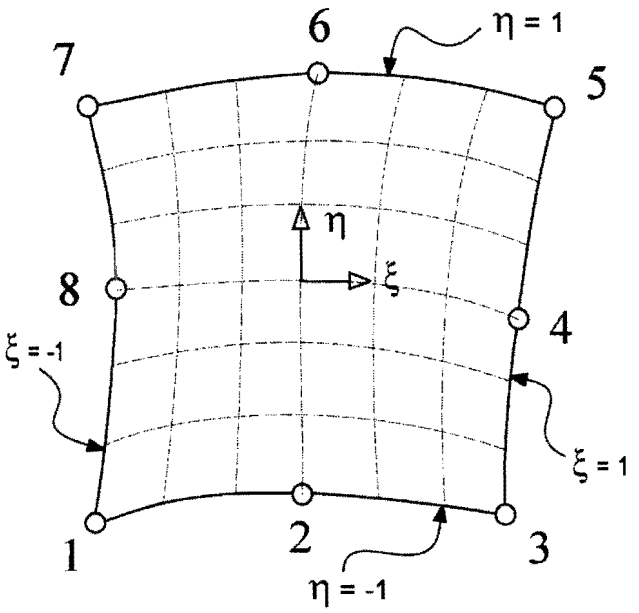

Figure 2-3: Element numbering

The geometry of each element is defined by

$$\begin{bmatrix} x(\xi,\eta) \\ y(\xi,\eta) \end{bmatrix} = \sum_{i=1}^{8} \begin{bmatrix} N_i & 0 \\ 0 & N_i \end{bmatrix} \begin{bmatrix} x_i \\ y_i \end{bmatrix} \tag{2.9}$$

where N_i is the parabolic shape function, or interpolation function, associated with node i. These functions have a value of unity at the associated nodes and zero at every other node.

Similarly the displacement field over the element is defined by

$$\boldsymbol{\delta} = \begin{bmatrix} w \\ \theta_x \\ \theta_y \end{bmatrix} = \sum_{i=1}^{8} \begin{bmatrix} N_i & 0 & 0 \\ 0 & N_i & 0 \\ 0 & 0 & N_i \end{bmatrix} \begin{bmatrix} w_i \\ \theta_{xi} \\ \theta_{yi} \end{bmatrix} \tag{2.10}$$

The shape functions are given by

$$
\begin{aligned}
N_1(\xi,\eta) &= -\frac{1}{4}(1-\xi)(1-\eta)(1+\xi+\eta) \\
N_2(\xi,\eta) &= \frac{1}{2}(1-\xi^2)(1-\eta) \\
N_3(\xi,\eta) &= \frac{1}{4}(1+\xi)(1-\eta)(\xi-\eta-1) \\
N_4(\xi,\eta) &= \frac{1}{2}(1+\xi)(1-\eta^2) \\
N_5(\xi,\eta) &= \frac{1}{4}(1+\xi)(1+\eta)(\xi+\eta-1) \\
N_6(\xi,\eta) &= \frac{1}{2}(1-\xi^2)(1+\eta) \\
N_7(\xi,\eta) &= \frac{1}{4}(1-\xi)(1+\eta)(-\xi+\eta-1) \\
N_8(\xi,\eta) &= \frac{1}{2}(1-\xi)(1-\eta^2)
\end{aligned}
\qquad (2.11)
$$

The variational approach to the formulation of the stiffness matrix is used, specifically the minimisation of potential energy principle. The potential energy functional consists of terms for bending, shear and external work done by the applied lateral pressure denoted by p:

$$\Pi = \frac{1}{2}\int_A \left(\{M\}^T\{\psi\} + \{Q\}^T\{\phi\}\right)dA - \int_A pwdA \qquad (2.12)$$

where {M} and {Q} are as defined in equations (2.15) and (2.16) respectively.

Positions of equilibrium are denoted by positions of stationary potential energy or $\delta\Pi = 0$, which leads to equation (2.30). The curvatures and shear strains are defined as

$$\{\psi\} = \begin{bmatrix} \psi_x \\ \psi_y \\ \psi_{xy} \end{bmatrix} = \begin{bmatrix} -\dfrac{\partial\theta_x}{\partial x} \\ -\dfrac{\partial\theta_y}{\partial y} \\ -\left(\dfrac{\partial\theta_x}{\partial y} + \dfrac{\partial\theta_y}{\partial x}\right) \end{bmatrix} \qquad (2.13)$$

$$\{\phi\} = \begin{bmatrix} -\phi_x \\ -\phi_y \end{bmatrix} \tag{2.14}$$

The stress resultants $\{M\}$ (bending moment) and $\{Q\}$ (shear force) are calculated by pre-integrating the relevant stresses over the depth of the plate which is denoted by h. The resultants are related to element strains by the following expressions, illustrated in the figure below:

$$\{M\} = \begin{bmatrix} M_x \\ M_y \\ M_{xy} \end{bmatrix} = [D_f]\{\psi\} \tag{2.15}$$

$$\{Q\} = \begin{bmatrix} Q_x \\ Q_y \end{bmatrix} = [D_s]\{\phi\} \tag{2.16}$$

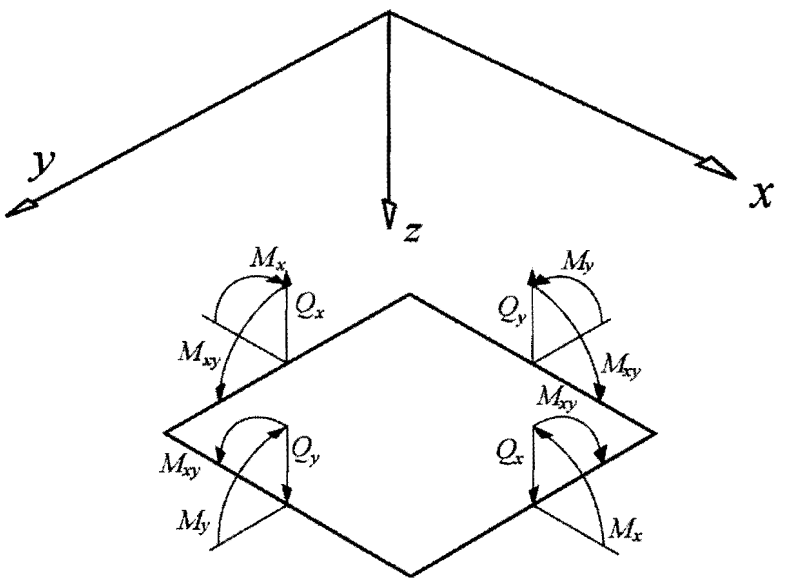

Figure 2-4: Sign convention (positive directions)

where $[D_f]$ and $[D_s]$ are the elasticity matrices,

$$[D_f] = \frac{Eh^3}{12(1-\nu^2)} \begin{bmatrix} 1 & \nu & 0 \\ \nu & 1 & 0 \\ 0 & 0 & \frac{1-\nu}{2} \end{bmatrix} \tag{2.17}$$

$$[D_s]=\frac{Eh\kappa}{2(1+\nu)}\begin{bmatrix}1 & 0\\ 0 & 1\end{bmatrix}=Gh\kappa\begin{bmatrix}1 & 0\\ 0 & 1\end{bmatrix} \tag{2.18}$$

for flexure and shear, respectively. The elasticity matrices above are usually combined as the total elasticity matrix:

$$[D]=\begin{bmatrix}\frac{E_c h^3}{12(1-\nu^2)} & \frac{E_c \nu h^3}{12(1-\nu^2)} & 0 & 0 & 0\\ \frac{E_c \nu h^3}{12(1-\nu^2)} & \frac{E_c h^3}{12(1-\nu^2)} & 0 & 0 & 0\\ 0 & 0 & \frac{Gh^3}{12} & 0 & 0\\ 0 & 0 & 0 & Gh\kappa & 0\\ 0 & 0 & 0 & 0 & Gh\kappa\end{bmatrix} \tag{2.19}$$

where $\kappa = 5/6$ is a shear correction factor, applicable only to rectangular sections. This factor is used to transform the assumed parabolic shear stress distribution over the depth of the plate to an equivalent constant stress distribution.

Strains are related to displacements by

$$\{\varepsilon\}=[L]\{\delta\} \tag{2.20}$$

where $\{\varepsilon\}$ is a generalised strain vector,

$$\{\varepsilon\}=\begin{bmatrix}\psi_x\\ \psi_y\\ \psi_{xy}\\ -\phi_x\\ -\phi_y\end{bmatrix} \tag{2.21}$$

$\{\delta\}$ is the generalised displacement vector and $[L]$ is the matrix of displacement differential operators. With the finite element method, $\{\delta\}$ is approximated by $N\delta^e$ within an element, where

$$[N]=\begin{bmatrix} N_1 & 0 & 0 & N_2 & 0 & 0 & . & 0 & 0 & N_8 & 0 & 0 \\ 0 & N_1 & 0 & 0 & N_2 & 0 & 0 & . & 0 & 0 & N_8 & 0 \\ 0 & 0 & N_1 & 0 & 0 & N_2 & 0 & 0 & . & 0 & 0 & N_8 \end{bmatrix} \tag{2.22}$$

and

$$\{\delta^e\}^T=[\delta_1 \quad \delta_2 \quad . \quad . \quad \delta_i \quad . \quad . \quad \delta_8] \tag{2.23}$$

is the vector of nodal displacement components and δ_i is given by

$$\{\delta_i\}=\begin{bmatrix} w_i \\ \theta_{xi} \\ \theta_{yi} \end{bmatrix} \tag{2.24}$$

Equation (2.20) then becomes

$$\{\varepsilon\}=[L][N]\{\delta^e\}=[B]\{\delta^e\} \tag{2.25}$$

where $[B]$ is known as the element strain matrix,

$$[B]=[B_1 \quad B_2 \quad . \quad . \quad B_i \quad . \quad . \quad B_8] \tag{2.26}$$

and $[B]_i$ is calculated for each node as

$$[B]_i=\begin{bmatrix} 0 & -\frac{\partial N_i}{\partial x} & 0 \\ 0 & 0 & -\frac{\partial N_i}{\partial y} \\ 0 & -\frac{\partial N_i}{\partial y} & -\frac{\partial N_i}{\partial x} \\ \frac{\partial N_i}{\partial x} & -N_i & 0 \\ \frac{\partial N_i}{\partial y} & 0 & -N_i \end{bmatrix} \tag{2.27}$$

Finally the element stiffness matrix can be assembled as

$$[K^e] = \iint [B]^T [D][B]\,dxdy = \iint [B]^T [D][B]|J|\,d\xi\,d\eta \qquad (2.28)$$

where $|J|$ is the determinant of the Jacobian matrix.

Distributed loads, denoted by p, must be represented as equivalent nodal loads in this method and the following equation is used for this purpose:

$$\{P_p^e\} = \int_{A_e} N_i p\,dA = \iint N_i p|J|\,d\xi\,d\eta \qquad (2.29)$$

where A_e is the elemental area.

The linear system of equations per element is then

$$\{P_p^e\} + \{P^e\} = [K^e]\{\delta^e\} \qquad (2.30)$$

where P^e denotes the nodal forces.

The element stiffness matrices are then assembled in the global stiffness matrix with the direct stiffness method and the problem reduces to a system of linear algebraic equations. This system can be solved with any suitable numerical method such as Gauss reduction or Cholesky decomposition.

A discussion on "shear locking", introduced at the beginning of the section, follows. Thin plates, modelled using Mindlin elements, often exhibit a high, incorrect shear stiffness which is termed shear locking. Mathematically this can be studied using the energy contributions of shear and flexure to equation (2.12). The flexural strain energy varies cubically with thickness whereas shear strain energy varies linearly, this implies that flexural strain energy decreases more rapidly with reductions in depth than shear strain energy.

When one takes into account that the shear strain energy is given by:

$$\Pi = \frac{1}{2}\int_A \left(\{\phi\}^T [D_s]\{\phi\}\right) dA \quad \text{and} \qquad (2.31)$$

$$[D_s] = Gh\kappa \begin{bmatrix} 1 & 0 \\ 0 & 1 \end{bmatrix} \qquad (2.32)$$

it appears that the shear strain energy should disappear as h→ 0. Due to the approximate nature of the finite element method, zero strain energy is rarely achieved and under various conditions, the stiffness matrix becomes ill-conditioned, Tesler & Hughes (1983), which leads to a gross overestimation of stiffness.

This locking problem can be avoided with the use of reduced or selective numerical integration (Zienkiewicz, Taylor and Too, 1971) . The basis of these integration schemes resides in the assumption that shear locking can be avoided by not integrating the shear strain energy exactly. This dissertation employs a reduced 2x2 Gaussian integration scheme.

Shear locking tendencies can be assessed using the constraint ratio, Hughes (1987), or the Kirchhoff mode concept, Hughes & Tezduyar (1981).

The entire analysis process for a linear-elastic analysis is illustrated in figure 7-1.

2.2 Cracked Sections

Concrete members crack when the tensile stress at a section exceeds the tensile strength, usually taken as the modulus of rupture for members subjected to flexure. The flexural stiffness along the member then varies between two extremes:

- Condition 1: Where the tensile stress is below the modulus of rupture, the concrete remains uncracked and the full section contributes to the stiffness.
- Condition 2: At sections where the tensile stress exceeds the modulus of rupture, the concrete cracks over the full depth of the tension zone. Cracks at these sections are often referred to as primary cracks. The flexural stiffness at such a cracked section can be estimated from the fully cracked, transformed section.

Assuming a stiffness based on condition 2 would overestimate the deflection of the member, since the regions between primary cracks remain uncracked or partially cracked. In these regions, the concrete in tension contributes to the flexural stiffness and this is referred to as tension stiffening.

Including tension stiffening in the deflection analysis of a concrete member involves interpolating between conditions 1 and 2. Two empirical methods are considered here, the Bilinear Method and Branson's Effective Moment of Inertia.

2.2.1 The Bilinear Method

This method, first proposed for beam cracking problems by Favre *et al* (1985), is developed below:

Assuming that plain sections remain plane in bending for uncracked and cracked sections, strains remain linearly distributed over the depth of a section. Although this is not strictly true at the cracked section, the *average* strain measured over a number of primary cracks retains proportionality to the distance from the neutral axis.

Subject to the assumption that no bond slip occurs, the strain in the tension reinforcement at uncracked sections (condition 1), just prior to cracking, can be expressed as:

$$\varepsilon_{s1} = \frac{M_r d_t}{I_1 E_c} \tag{2.33}$$

where M_r is the cracking moment at the section under consideration, d_t is the depth from the neutral axis of the section to the level of the tension reinforcement, I_1 is the moment of inertia based on the uncracked transformed section and E_c is the secant modulus of elasticity of the concrete.

The cracking moment for a rectangular section can be expressed as

$$M_r = \frac{f_r I_g}{h/2} \tag{2.34}$$

where f_r is the modulus of rupture, I_g is the moment of inertia of the gross concrete section neglecting reinforcement and h is the section depth.

At fully cracked sections (condition 2), equation (2.33) changes to

$$\varepsilon_{s2} = \frac{Md_t}{I_2 E_c} \tag{2.35}$$

where I_2 is the moment of inertia based on the fully cracked transformed section and $M \geq M_r$. The steel stresses for condition 1 and 2 would then be

$$\sigma_{s1} = E_s \varepsilon_{s1} \tag{2.36}$$

$$\sigma_{s2} = E_s \varepsilon_{s2} \tag{2.37}$$

assuming linear elastic reinforcement behaviour as illustrated in figure 2-5.

Between primary cracks, the reinforcement strain increases to a value larger than ε_{s1} but smaller than ε_{s2}. The steel strain will gradually decrease from its maximum value at the crack to ε_{s1} as bond transfers tension from the reinforcement to the concrete. When the strain reaches ε_{s1}, another primary crack forms and the process repeats itself.

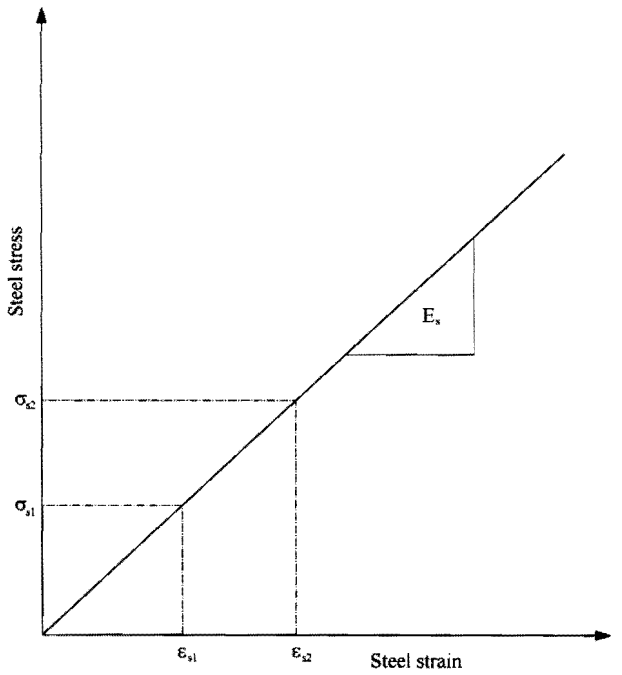

Figure 2-5: Reinforcement stress-strain relation

Let ε_{sm} represent the mean strain of the reinforcement in the member

$$\varepsilon_{sm} = \frac{\Delta l}{l} \tag{2.38}$$

where Δl is the change in member length at the level of the reinforcement and l the original length. As mentioned in the preceding paragraph ε_{sm} will be smaller than ε_{s2} with the difference $\Delta\varepsilon_s$, thus

$$\varepsilon_{sm} = \varepsilon_{s2} - \Delta\varepsilon_s \tag{2.39}$$

This difference has a maximum value of $\Delta\varepsilon_{smax}$ at the onset of cracking. Experimental evidence has shown that $\Delta\varepsilon_s$ can be related to σ_{s2} as follows, Ghali & Favre (1986)

$$\Delta\varepsilon_s = \Delta\varepsilon_{s\,max}\frac{f_r}{\sigma_{s2}} = \Delta\varepsilon_{s\,max}\frac{M_r}{M} \tag{2.40}$$

Note that equation (2.40) is based on the assumption that the uncracked concrete has the same effect on the mean reinforcement strain in flexure as is the case with axial loading.

Equations (2.39) and (2.40) are shown graphically in figure 2-6 below.

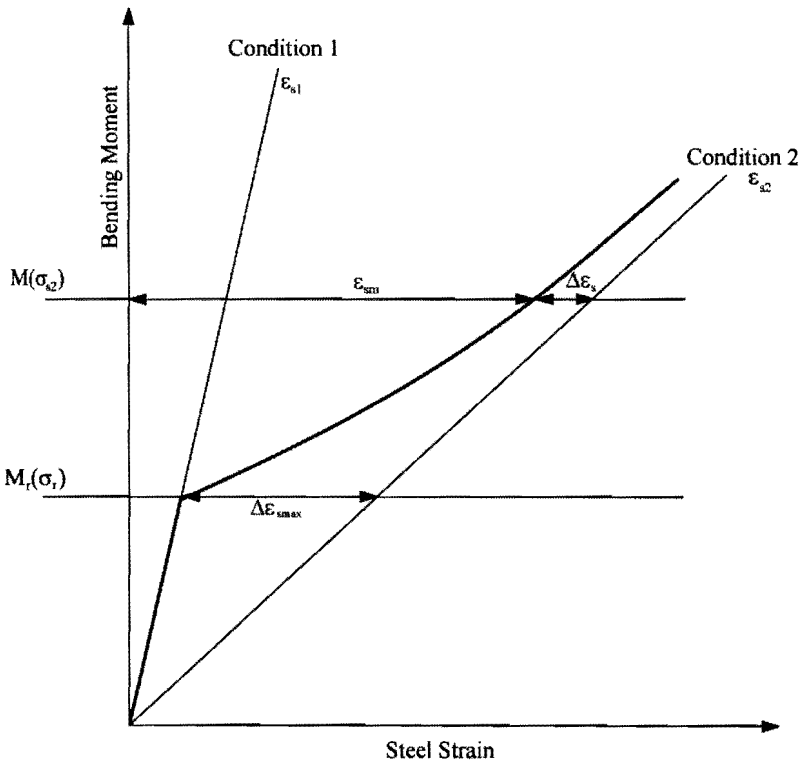

Figure 2-6: Variation of steel strains versus bending moment

From the geometry of the graph, $\Delta\varepsilon_{smax}$ can be written as

$$\Delta\varepsilon_{s\max} = (\varepsilon_{s2} - \varepsilon_{s1})\frac{M_r}{M} \tag{2.41}$$

Substituting equation (2.41) and (2.40) into equation (2.39) yields

$$\varepsilon_{sm} = (1-\zeta)\varepsilon_{s1} + \zeta\varepsilon_{s2} \quad \text{or} \tag{2.42}$$

$$\psi_{sm} = (1-\zeta)\psi_{s1} + \zeta\psi_{s2} \tag{2.43}$$

where ζ is a dimensionless parameter that measures the extent of cracking, zero for an uncracked section and between zero and unity for a fully cracked section. The parameters ψ_{s1} and ψ_{s2} represent the curvatures at the uncracked and cracked states, respectively.

$$\zeta = 1 - \left(\frac{M_r}{M}\right)^2 \quad \text{with } M > M_r \tag{2.44}$$

The CEB-FIP Model Code 1990 (1993) introduces two additional parameters to account for the difference in bond characteristics of deformed and plain bars, as well as long term effects

$$\zeta = 1 - \beta_1\beta_2\left(\frac{M_r}{M}\right)^2 \tag{2.45}$$

β_1 equals 1 and 0.5 for deformed and plain bars, respectively. β_2 equals 1 and 0.5 for immediate loading and sustained loading, respectively.

This approach to tension stiffening can be used in combination with the hand-calculation method described in section 2.1.1. A curvature coefficient is calculated for condition 1 and 2:

$$\kappa_{s1} = \frac{I_g}{I_1} \tag{2.46}$$

$$\kappa_{s2} = \frac{I_g}{I_2} \tag{2.47}$$

These coefficients represent the influence of the reinforcement on uncracked and cracked curvatures.

An effective coefficient is then found by interpolating with equation (2.44):

$$\kappa_s = (1-\zeta)\kappa_{s1} + \zeta\kappa_{s2} \tag{2.48}$$

where:

I_g = Moment of inertia of the gross concrete area, neglecting reinforcement;

I_1 = Moment of inertia of the uncracked, transformed section;

I_2 = Moment of inertia of the fully cracked transformed section;

κ_{s1} = Curvature coefficient for condition 1;

κ_{s2} = Curvature coefficient for condition 2.

2.2.2 Branson's Effective Moment of Inertia

Similar to the bilinear method, this method proposes an effective moment of inertia, constant over the length of a member, for the computation of deflections. The effective moment of inertia, developed by Branson (1968), is expressed as:

$$I_e = \left(\frac{M_r}{M}\right)^m I_g + \left[1-\left(\frac{M_r}{M}\right)^m\right] I_2 \tag{2.49}$$

where I_g is the moment of inertia of the gross concrete section neglecting reinforcement and m is a power usually set to 3, although Branson suggested a value of 4 for calculating I_e at a specific section.

Although this equation was developed for beams, a study undertaken by Polak (1996), suggests that sufficiently accurate deflection results are achieved for slabs using the equation in conjunction with the finite element method. This method is set out below.

The difficulty in applying Branson's equation to plate bending problems concerns the definition of flexural rigidity. In the case of beams the flexural rigidity is simply the product EI, whereas in the plate formulation, flexural rigidity is represented by the matrix $[D_f]$ as shown in equation (2.17). Polak circumvented this difficulty by modifying E and ν instead of I.

The ratio of the cracked to gross second moments of inertia is used to modify $[D]$ per element. This implies that the cracked section properties are averaged across all nodes belonging to an element to

arrive at a single partially cracked element. This is achieved by calculating average moments in the x and y-directions for use in equation (2.49),

$$M_{xavg} = \frac{1}{n}\sum_{i=1}^{n}\left(|M_{xi}| + |M_{xyi}|\right) \tag{2.50}$$

$$M_{yavg} = \frac{1}{n}\sum_{i=1}^{n}\left(|M_{yi}| + |M_{xyi}|\right) \tag{2.51}$$

where n is the number of Gaussian sampling points and M_{xi}, M_{yi} are the moments calculated at sampling point i.

The elasticity matrix, modified for tension stiffening, takes the following orthotropic form:

$$[D] = \begin{bmatrix} \frac{E_x h^3}{12(1-\nu_x\nu_y)} & \frac{E_y\nu_x h^3}{12(1-\nu_x\nu_y)} & 0 & 0 & 0 \\ \frac{E_x\nu_y h^3}{12(1-\nu_x\nu_y)} & \frac{E_y h^3}{12(1-\nu_x\nu_y)} & 0 & 0 & 0 \\ 0 & 0 & \frac{G_1 h^3}{12} & 0 & 0 \\ 0 & 0 & 0 & G_2 h & 0 \\ 0 & 0 & 0 & 0 & G_3 h \end{bmatrix} \tag{2.52}$$

where:

$$E_x = \alpha_x E_c, \qquad E_y = \alpha_y E_c \tag{2.53}$$

$$\nu_x = \alpha_x \nu, \qquad \nu_y = \alpha_y \nu \tag{2.54}$$

$$G_1 = G\alpha_x\alpha_y, \quad G_2 = G\alpha_x, \quad G_3 = G\alpha_y \tag{2.55}$$

$$\alpha_x = \frac{I_{ex}}{I_g}, \qquad \alpha_y = \frac{I_{ey}}{I_g} \tag{2.56}$$

I_{ex} and I_{ey} are calculated using the average moments obtained from equations (2.50) and (2.51).

Bensalem (1997) pointed out weaknesses in Polak's proposed method, many of which are intentional approximations with a simple method in mind as pointed out in Polak's closure.

One of these weaknesses involves the calculation of the average moments. Bensalem argues that the approach would only be valid for conditions when the signs of the moments are the same. Should these signs differ, over- or underestimation of the average moments would occur. Typical rectangular layouts lead to same sign moments and the approach remains valid.

The analysis algorithm, as given by Polak, is restated in simplified form in figure 7-2 for reference.

2.2.3 Rigorous methods

A number of sophisticated approaches to post-cracking behaviour and tension stiffening have been proposed. These models usually incorporate non-linear constitutive relations and multi-layer elements as the main components.

Chan et al (1994), utilises strain hardening plasticity theory to develop the constitutive model for a finite element analysis and also present a bond stress distribution function to model tension stiffening. Principal stresses at integration points are evaluated and compared to the cracking strength of the concrete. Should the cracking strength be exceeded, tangential concrete moduli are calculated using the bond stress distribution. The constitutive matrix is modified with the tangential moduli and the analysis proceeds in an iterative manner with continuous model updating.

Hu et al (1991), use a similar approach as above, except that an explicit tension stiffening function and a layered finite element formulation is used. Crack directions are modified during the analysis to ensure that cracks remain normal to the maximum principal stresses.

Due to the non-linear nature of the methods briefly outlined above, and in fact almost all sophisticated methods, iteration, and all the associated numerical difficulties, is required. Large finite element models using these approaches become bulky in terms of storage requirements and computing time.

2.3 Creep

Creep is a progressive increase in strain under sustained loading and is responsible for the largest portion of long term deflections in concrete structures. The current state of the art with regards to creep is perhaps best described in a paper by Bažant (2001) : "...despite major successes, the

phenomenon of creep and shrinkage is still far from being completely understood, even though it has occupied some of the best minds in the field on cement and concrete research and material science…"

A large number of predictive physical models have been proposed in the past and are still being developed. Neville & Dilger (1970) and Bažant (2001) have provided detailed overviews of these models and they will not be repeated here.

These physical models lead to mathematical models that facilitate structural analysis:

- Effective modulus method.
- Age-adjusted effective modulus method.
- Rate of creep method.
- Improved Dischinger method.
- Rheological models.

Analysis methods fall into two classes:

- Single step approximations.
- Step-by-step iterative solutions.

Of these, the simplest choice would be the age-adjusted effective modulus method using a single time-step approximation. These single step approximations yield acceptable upper bound deflections for routine design and are not plagued with the numerical problems of iterative rheological approaches, such as creep divergence, Bažant (1993).

The discussion below is therefore limited to the effective modulus method and the related age-adjusted effective modulus method.

In the study of creep effects, it is convenient to separate creep strain into the following components (figure 2-7):

- Irrecoverable creep or flow, designated by ε_f.
- ε_f is further divided into basic creep and drying creep.
- Recoverable creep or delayed elastic strain, designated by ε_d.

One of the main disadvantages of the effective modulus method is its inability to deal with decreasing stress histories. As can be seen from figure 2-7, creep involves a measure of irrecoverable strain. The

effective modulus method, due to its elastic nature, predicts complete recovery of creep strains, i.e. a return to zero strain at unloading. This will lead to a severe underestimation of deflection for structures subjected to cyclic loading.

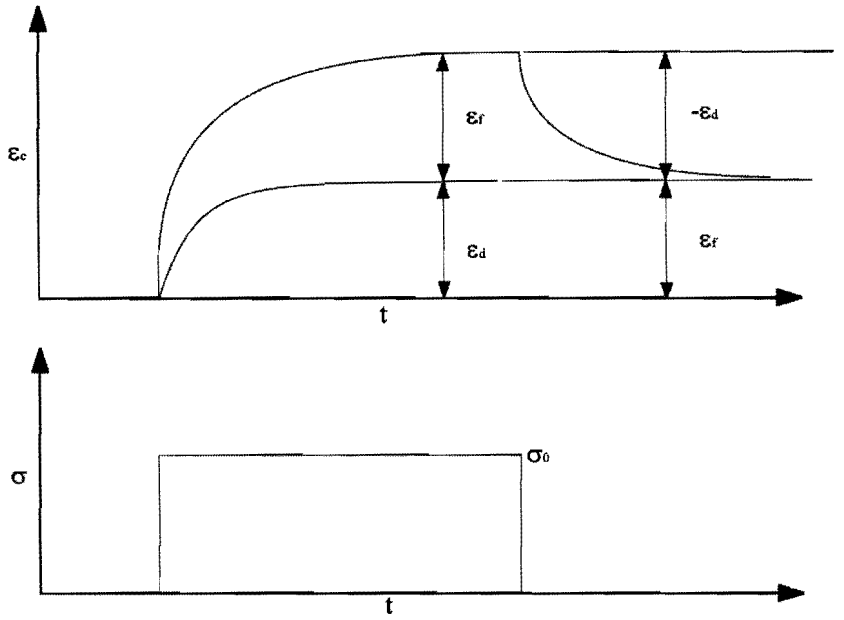

Figure 2-7: Creep components due to a load pulse

The total creep potential of a concrete specimen is usually described by a creep coefficient, $\phi(t,\tau)$, which is expressed as,

$$\phi(t,\tau) = \frac{\varepsilon_c(t)}{\varepsilon_e} \tag{2.57}$$

where:

$\varepsilon_c(t)$ = Creep strain at time t.

ε_e = Instantaneous elastic strain.

τ = Age at loading.

This coefficient increases with time and is highly dependent on the concrete maturity at first loading. One of the largest uncertainties in creep problems is the magnitude of ϕ. A vast number of procedures are available for the calculation of ϕ, many of which calculate contributing portions to ϕ for the various components of the total creep strain.

The effective modulus method involves replacing the modulus used in the analysis with an artificial, effective modulus:

$$E_e(t,\tau) = \frac{E_c}{1+\phi(t,\tau)} \tag{2.58}$$

where:

$E_e(t,\tau)$ = Effective modulus at time t for a specimen loaded at time τ.

E_c = Concrete modulus of elasticity at time zero.

Equation (2.58) allows the calculation of total deflection at time t, If only the creep increment in deflection is sought, equation (2.58) becomes:

$$E_e(t,\tau) = \frac{E_c}{\phi(t,\tau)} \tag{2.59}$$

The age-adjusted method allows an improved estimation of ϕ. Since the full loading is rarely instantaneously applied at time τ, as suggested by figure 2-7, the total load causing deflection is only active at some time later than τ. As mentioned earlier, ϕ is very sensitive to τ and should therefore be modified to account for this gradual increase in load. The age-adjusted method suggests the use of a factor, $\chi(t,\tau)$ smaller than unity, to reduce the magnitude of ϕ.

Equation (2.58) then becomes,

$$E_e(t,\tau) = \frac{E_c}{1+\chi(t,\tau)\phi(t,\tau)} \tag{2.60}$$

As for ϕ, various national building codes suggest procedures for the calculation of $\chi(t,\tau)$. For the purposes of this dissertation it is assumed that ϕ and χ are known and the focus falls on the implementation of these quantities in a creep analysis.

The method set out below is often referred to as the "Section Curvature Method" and is taken from Ghali and Favre (1986). The equation variables are illustrated in figure 2-8.

The creep curvature increment of a plain concrete member subjected to flexure and assumed to be uncracked may be expressed as:

$$\Delta\psi = \phi(t,\tau)\psi_e \qquad (2.61)$$

where:

$\Delta\psi$ = Creep increment in curvature;

$\phi(t,\tau)$ = Creep coefficient at time t for loading at time τ;

ψ_e = Elastic curvature at time τ.

Similar to equation (2.57), equation (2.61) modifies the elastic curvature for creep, based on the creep coefficient and the assumption that strain is linearly related to curvature.

Reinforcement tends to restrict concrete creep and the magnitude of this influence is a function of section geometry and reinforcement ratio. The effect of reinforcement on concrete creep can be expressed by a dimensionless parameter κ_c, as shown in equation (2.62):

$$\Delta\psi = \kappa_c\left[\phi(t,\tau)\left(\psi_e + \varepsilon_O\frac{y_c}{r_c^{\,2}}\right)\right] \qquad (2.62)$$

where:

κ_c = Creep curvature coefficient, defined by equation (2.64);

ε_O = Axial strain at point O at time τ, point O is a reference point chosen at the centroid of the age adjusted transformed section;

y_c = y-coordinate of the centroid of A_c at time τ, measured downwards from the centroid of the age-adjusted transformed section.

$r_c^{\,2}$ = I_c/A_c

I_c = Moment of inertia of A_c about an axis through the centroid of the age-adjusted transformed section.

A_c = Effective concrete area, full area for uncracked sections and the concrete compression zone for cracked members.

This dissertation neglects the effect of membrane action in the slab and equation (2.62) can then be simplified to:

$$\Delta\psi = \kappa_c\left[\phi(t,\tau)\psi_e\right] \tag{2.63}$$

The parameter κ_c can be calculated from:

$$\kappa_c = \frac{I_c + A_c y_c \Delta y}{\bar{I}} \tag{2.64}$$

where:

Δy = y-coordinate of the centroid of the age adjusted transformed section, measured downwards from the centroid of the transformed section at time τ.

$\bar{I}$ = Moment of inertia of the age adjusted transformed section about an axis through its centroid.

Figure 2-8, taken from Ghali & Favre, illustrates the variables used in equations (2.62) to (2.64). This approach is applied to the finite element method in section 3.2.

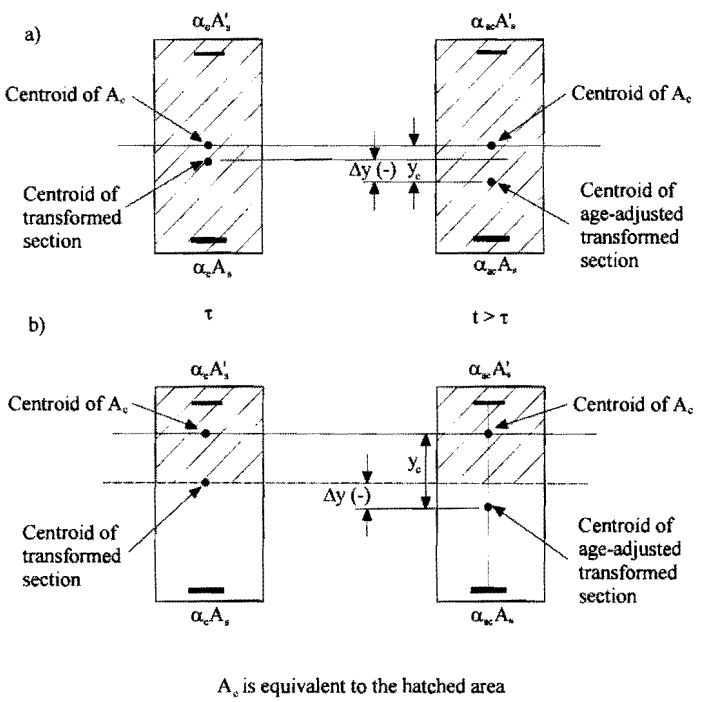

Figure 2-8: Creep section parameters for a) uncracked section; b) cracked section

(Reproduced from Ghali & Favre (1986))

2.4 Shrinkage

Shrinkage occurs when a hygral gradient exists between a concrete member and the surrounding environment. Pore and adsorbed water migrates from the concrete and causes a change in volume. Should this change in volume be restrained by reinforcement or support conditions, tensile stresses develop which could in turn cause cracking. When free shrinkage, denoted by ε_{cs}, is restrained by an unsymmetrical arrangement of reinforcement about the neutral axis of a member, an increase in curvature occurs.

The derivation below is taken from Kong & Evans (1987).

From basic theory, the shrinkage curvature can be written as,

$$\psi = \frac{\varepsilon_2 - \varepsilon_1}{d} \tag{2.65}$$

From the geometry of figure 2-9,

$$\varepsilon_2 = \varepsilon_{cs} - \frac{f_{c2}}{E_c} \quad \text{and} \tag{2.66}$$

$$\varepsilon_1 = \varepsilon_{cs} - \frac{f_{c1}}{E_c} \tag{2.67}$$

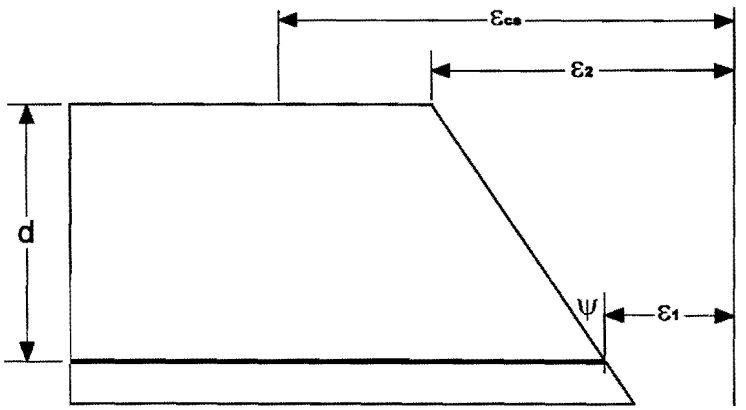

Figure 2-9: Shrinkage strains in a singly reinforced member

From the requirements of equilibrium,

$$f_{c1} = \frac{(f_s A_s)}{A} - \frac{(f_s A_s) e_s}{I}(d - e_s) \text{ and} \tag{2.68}$$

$$f_{c2} = \frac{(f_s A_s)}{A} + \frac{(f_s A_s) e_s}{I} e_s \tag{2.69}$$

where:

f_s = Steel stress due to shrinkage ($E_s \epsilon_1$);

f_{c1} = Concrete tensile stress at the tension reinforcement level due to shrinkage;

f_{c2} = Concrete tensile stress at the top fibre of the section due to shrinkage;

e_s = Eccentricity of the steel centroid with respect to the centroid of the transformed section;

A = Concrete cross sectional area;

A_s = Area of reinforcement;

I = Moment of inertia of the age-adjusted transformed section.

Equation (2.65) can then be rewritten as:

$$\psi_{sh} = \frac{\varepsilon_{cs} \alpha_e A_s e_s}{I} \tag{2.70}$$

where α_e is defined as

$$\alpha_e = \frac{E_s}{E_c} \tag{2.71}$$

It should be noted that α_e is based on the effective concrete modulus and I is based on the age-adjusted transformed section.

Equation (2.70) holds for singly reinforced uncracked members, and very little error is involved by applying the equation to cracked sections as well (Kong & Evans, 1987).

This approach for singly reinforced sections is applied to the finite element method in section 3.3.